Effect of Nanoscale Fully Vulcanized Acrylic Rubber Powders on Crystallization of Poly(butylene terephthalate): Nonisothermal Crystallization

Jiann-Wen Huang

Department of Styling and Cosmetology, Tainan University of Technology, Yung Kang City, 710 Taiwan, Republic of China

Received 14 March 2007; accepted 24 May 2007
DOI 10.1002/app.26859
Published online 20 July 2007 in Wiley InterScience (www.interscience.wiley.com).

ABSTRACT: Poly(butylene terephthalate) (PBT) was blended with different content (1, 3, and 6 wt %) of nanoscale fully vulcanized acrylic rubber (FVAR) powders in a twin extruder to prepare PBT/FVAR composites (PBT/FVAR1, PBT/FVAR3, and PBT/FVAR6).The influence of different content (1, 3, and 6 wt %) of nanoscale FVAR powder on the nonisothermal crystallization behavior of PBT was investigated by using differential scanning calorimeter. The nonisothermal crystallization data were analyzed using Avrami, Ozawa, and Liu-Mo methods. The validity of kinetic models on the nonisothermal crystallization process of PBT and PBT/FVAR blends was discussed. All kinetic parameters showed that the ''crystallization rate'' followed the order: PBT > PBT/FVAR1 > PBT/FVAR3 > PBT/FVAR6 at a given cooling rate during experimental crystallization. However, when undercooling was taken into consideration, crystallization ability followed the order: PBT > PBT/FVAR6 > PBT/FVAR3 > PBT/FVAR1. A modified the Lauritzen–Hoffman equation was used to derive nucleation parameter (K_g) derived from nonisothermal crystallization. The results revealed that FVAR particles hindered the crystallization; however higher content of FVAR powders acted as heterogeneous nuclei in the nucleation stage to facilitated the crystallization of PBT. The dependence of the effective activation energy on conversion was evaluated on the basis of Friedman equation. © 2007 Wiley Periodicals, Inc. J Appl Polym Sci 106: 2031–2040, 2007

Key words: poly(butylene terephthalate); nonisothermal crystallization; elastomeric nanoparticles

INTRODUCTION

Poly(butylene terephthalate), PBT, is a semicrystalline thermoplastic polymer with good combination of properties, such as rigidity, solvent resistance, and rates of crystallization that allow short cycle time in injection molding.[1] But low impact strength has restricted their applications. Many tougheners have been added to PBT to enhance its impact property such as poly(ethylene octene),[2] poly(acrylonitrile-*co*-butadiene-*co*-styrene),[3–6] ethylene–propylene–diene,[7] ethylene–propylene rubber[8,9] and poly(ethylene-*co*-glycidyl methacrylate).[10]

A new kind of highly cross-linked nanoparticle rubbers, ultra-fine full-vulcanized rubber powders with particle size between 30 and 2000 nm has been applied in toughening the polymers.[11,12] When the particle size is below 100 nm, the ultra-fine full-vulcanized rubber powders can be also recognized as elastomeric nanoparticle. According to the toughening theory,[13] the brittle–tough transition occurs at a very low rubber volume fraction if the particle size of rubber is small enough.

In our previous work,[14] nanoscale fully vulcanized acrylic rubber (FVAR) particles were compounded in PBT and showed good dispersion from SEM micrographs. Those FVAR particles affect the isothermal crystallization, which was also simulated by kinetic models. The FVAR could be blended with thermoplastic polymers by standard plastic compounding machinery and applied in many fields.[11,12] The FVAR can greatly improve toughness of many polymers,[11,12,14] and at the same time it can keep the stiffness and/or heat resistance of plastics not only from lowering but also increasing substantially.[11] Research on polymer crystallization is limited to idealized conditions such as isothermal crystallization with constant external conditions; therefore, the theoretical analysis is relatively easy. Practically, however, the crystallization in a continuously varying environment is of great interest because industrial processes, such as injection molding of connectors, generally proceed under nonisothermal conditions.

In this article, nonisothermal crystallization of PBT and PBT/FVAR blends were studied by DSC and several nonisothermal crystallization models were used to describe the crystallization process. In addition, the

Correspondence to: J.-W. Huang (jw.huang@msa.hinet.net).

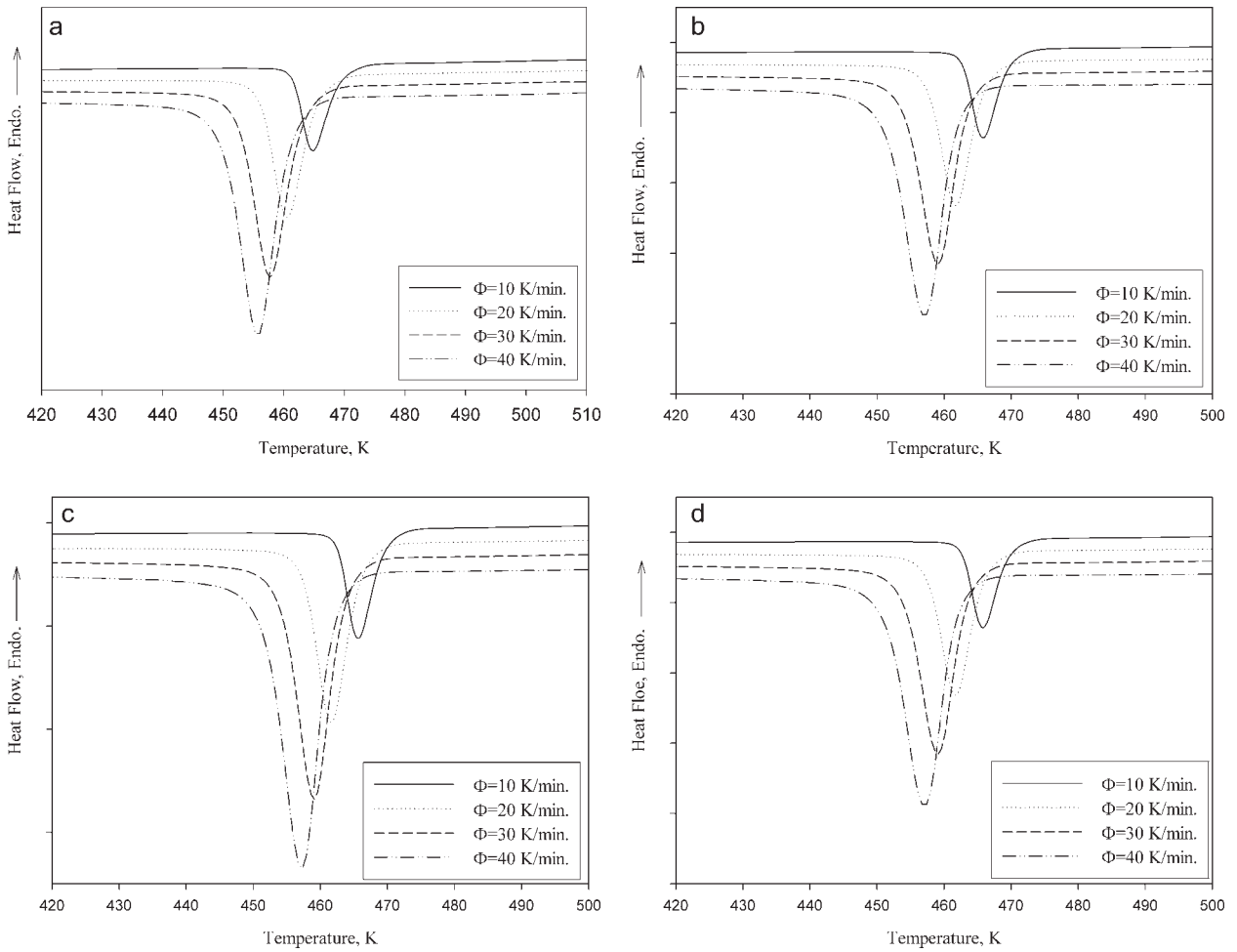

Figure 1 DSC nonisothermal measurement curves for PBT and PBT/FVAR blends. (a) PBT, (b) PBT/FVAR1, (c) PBT/FVAR3, (d) PBT/FVAR6.

undercooling, nucleation parameters and activation energies of crystallization were also discussed.

EXPERIMENTAL

Materials

Commercial grade PBT was supplied by ChangChun Group (trade name: 2000-201D, Taipei, Taiwan)) with a melt flow index (MFI) of 18–22 g/10 min. (235°C × 2.16 kgf, ASTM D 1238). FVAR powder (trade name: VP-301) with particle size of 50–100 nm was offered by Beijing Research Institute of Chemical Industry, SINOPEC, China. All materials were used as received without purification.

Sample preparation

All materials were dried at 373 K in a vacuum oven for 6 h before compounding. PBT was compounded with FVAR powder in a twin-screw extruder (Continent

TABLE I
Characteristic Data of Nonisothermal Melt Crystallization Exotherms for PBT and PBT/FVAR Blends

Sample	Cooling Rate (K/min)	T_o (K)	T_p (K)	$T_{1/2}$ (K)	$t_{1/2}$ (min)
PBT	10	472.2	464.7	465.2	0.706
	20	469.9	460.7	460.7	0.461
	30	468.6	457.7	457.7	0.362
	40	467.2	455.4	455.4	0.295
PBT/FVAR1	10	474.7	465.8	466.1	0.866
	20	472.5	461.6	461.7	0.541
	30	470.5	459.2	458.8	0.391
	40	469.2	456.7	456.6	0.317
PBT/FVAR3	10	474.9	465.6	465.9	0.896
	20	472.8	461.6	461.7	0.559
	30	472.0	459.1	458.8	0.440
	40	470.5	457.3	456.7	0.346
PBT/FVAR6	10	475.1	464.5	465.3	0.976
	20	472.9	460.1	460.7	0.559
	30	472.0	457.7	457.7	0.478
	40	471.2	455.4	455.3	0.396

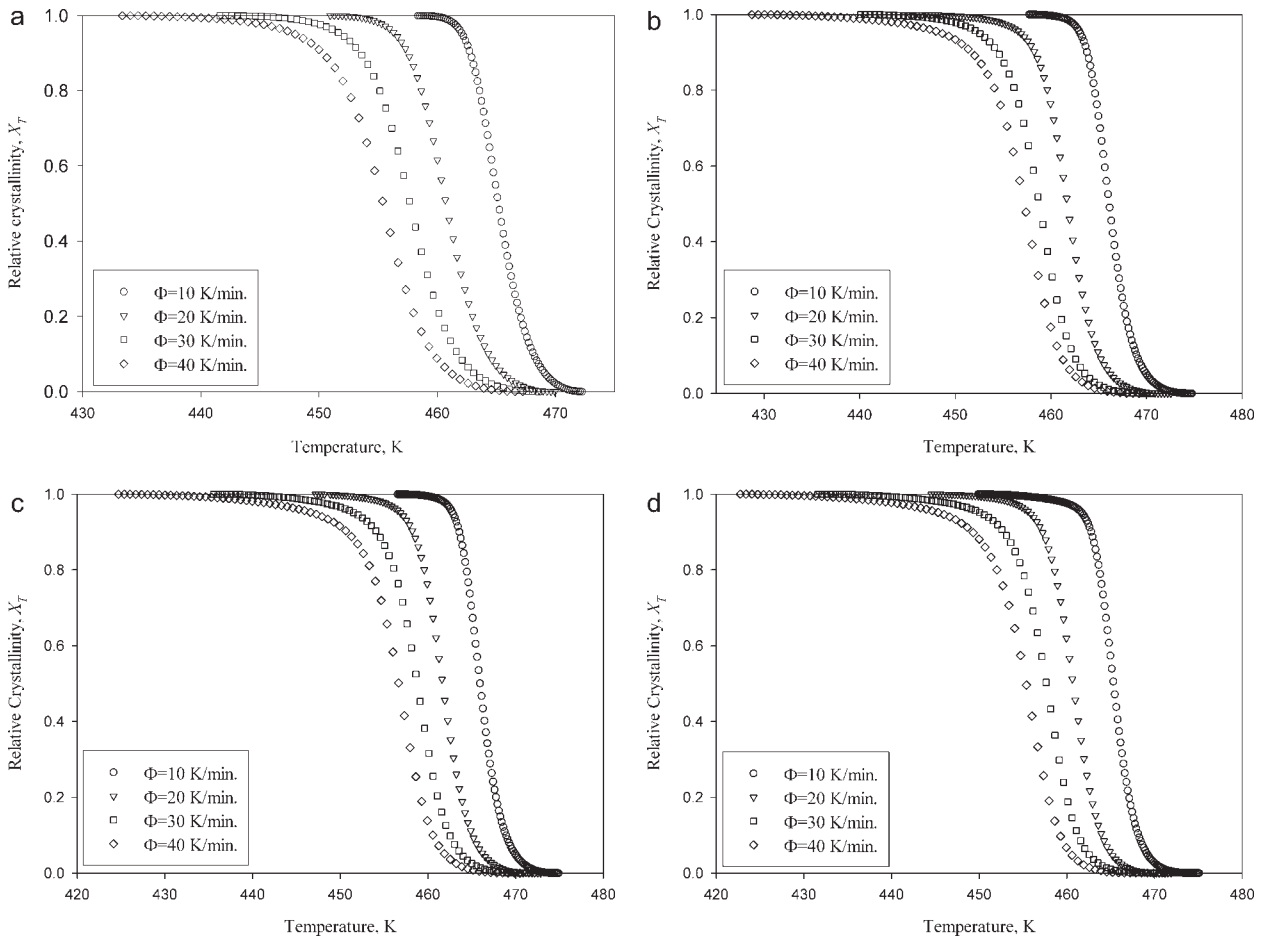

Figure 2 Experimental relative crystallinity as a function of temperature at different cooling rate. (a) PBT, (b) PBT/FVAR1, (c) PBT/FVAR3, (d) PBT/FVAR6.

Machinery Company, Model CM-MTE, L/D=32, D = 40 mm) at 623 K and 100 rpm to prepare PBT/FVAR blends. FVAR contents were 1 wt % (PBT/FVAR1), 3 wt % (PBT/FVAR3), and 6 wt % (PBT/FVAR6). Neat PBT also went through similar thermal history.

Characterizations

The nonisothermal crystallization behaviors of polymer blends were investigated with a differential scanning calorimeter, Perkin–Elmer DSC-1. The differential scanning calorimeter was calibrated using indium with samples weights of 8–10 mg. All operations were carried out in a nitrogen atmosphere. Before the data gathering, the samples were heated to 583 K and held in the molten state for 5 min to eliminate the influence of thermal history. The sample melts were then subsequently cooled to 308 K at a cooling rate of 10, 20, 30, and 40 K/min.

RESULTS AND DISCUSSION

In previous study,[14] FVAR particles were dispersed well and hardly distinguishable from the PBT matrix in PBT/FVAR blends under scanning electron microscope (SEM) observation. The addition of FVAR particles affects the isothermal crystallization of PBT.

Figure 1 shows representative DSC scans of PBT and FVAR-filled PP blends on cooling from 583 K at various cooling rates. The cooling rate dependence of the onset (T_o) and peak (T_p) of the crystallization exotherms were shown in Table I. It was observed that both T_o and T_p decreased with increasing cooling rate. Crystallization started at higher temperatures when cooling rate was lower, because there was more time to overcome the nucleation energy barriers; while at higher cooling rate the nuclei become active at lower temperature.[15] The presence of FVAR in PBT led to an increase in T_o at a given cooling rate because FVAR acted as a nucleating agent and therefore PBT in PBT/FVAR blends started to crystallize earlier.

The relative crystallinity as a function of temperature, X_T, was calculated as the ratio of the exothermic peak areas.[16,17]

$$X_T = \frac{\int_{T_o}^{T} \left[\frac{dH_c}{dT}\right] dT}{\int_{T_o}^{T_\infty} \left[\frac{dH_c}{dT}\right] dT} \quad (1)$$

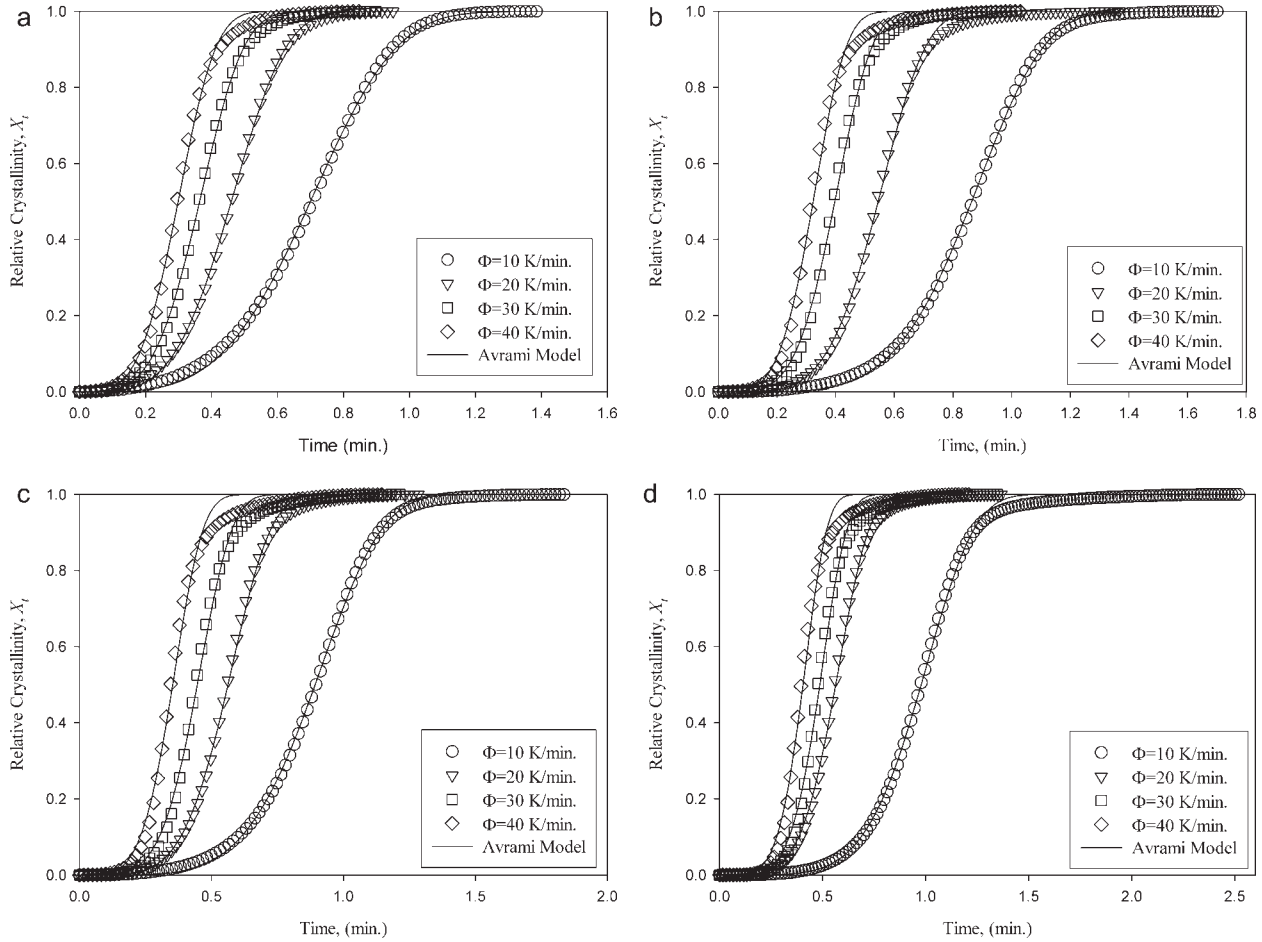

Figure 3 Experimental relative crystallinity as a function of time at different cooling rate and Avrami analysis. (a) PBT, (b) PBT/FVAR1, (c) PBT/FVAR3, (d) PBT/FVAR6.

where T is an arbitrary temperature, dH_c is the enthalpy of crystallization released during an infinitesimal temperature interval dT; Figure 2(a–d) present the relative crystallinity (X_T) as a function of temperature for PBT and PBT/FVAR blends. The temperature abscissa in Figure 2 could be transformed into a time scale, as shown in Figure 3, based on the following equation:

$$t = \left| \frac{T_o - T}{\Phi} \right| \tag{2}$$

where Φ is cooling rate. The relative crystallinity (X_t) of PBT and PBT/FVAR blends as a function of time were illustrated in Figure 3(a–d). It can be seen clearly from Figure 3 that the higher the cooling rate, the shorter the time for completing the crystallization.

Table I also shows the half-time of crystallization ($t_{1/2}$), defined as the time from the onset of crystallization to the time at which X_t is 50%. The inverse value of $t_{1/2}$ (i.e., $1/t_{1/2}$) signifies the bulk crystallization rate and a lower $1/t_{1/2}$ value indicates slower crystallization. The $t_{1/2}$ value decreased with increasing cooling rate indicating the polymer crystallized faster when the cooling rate was increased. At a given cooling rate, the $t_{1/2}$ for PBT and PBT/FVAR blends followed the order: PBT/FVAR6 > PBT/FVAR3 > PBT/FVAR1 > PBT implying that the

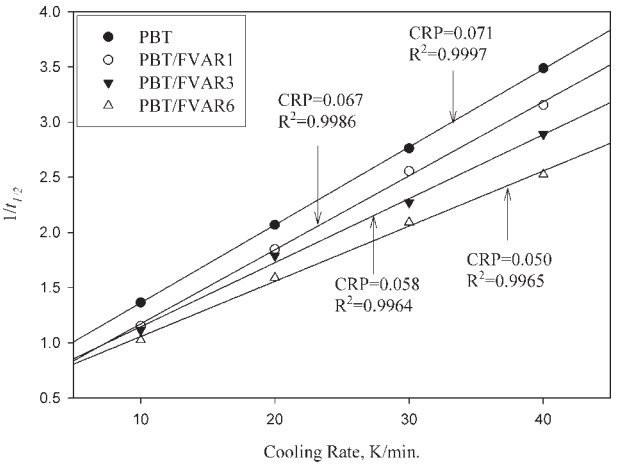

Figure 4 Plots of reciprocal half-time of crystallization as a function of cooling rate for PBT and PBT/FVAR blends.

TABLE II
Avrami Kinetics Parameters

Sample	Cooling rate (K/min)	n_a	K_a	K_J	R^2
PBT	10	3.86	1.2998	1.0266	0.9994
	20	3.96	1.8830	1.0321	0.9997
	30	3.90	2.7018	1.0337	0.9992
	40	3.76	3.9375	1.0349	0.9984
PBT/FVAR1	10	4.92	1.0757	1.0073	0.9998
	20	4.73	1.6003	1.0238	0.9995
	30	4.43	2.3220	1.0285	0.9984
	40	4.11	3.2339	1.0298	0.9983
PBT/FVAR3	10	4.97	1.0407	1.0040	0.9998
	20	4.88	1.4500	1.0188	0.9996
	30	4.80	2.0756	1.0246	0.9988
	40	4.38	2.9056	1.0270	0.9959
PBT/FVAR6	10	5.32	0.9545	0.9954	0.9993
	20	4.91	1.3470	1.0150	0.9990
	30	5.16	1.9156	1.0219	0.9973
	40	4.94	2.4921	1.0231	0.9959

crystallization rate followed the order: PBT > PBT/FVAR1 > PBT/FVAR3 > PBT/FVAR6. The overall crystallization rate is governed by nucleation and diffusion.[18] Nanoscale FVAR particles have shown to act as nucleating agent to increase the nucleation rate; however, the FVAR also hinders the crystallization under nonisothermal conditions by slowing down the diffusion of PBT chains.[19–22]

The slope of $1/t_{1/2}$ versus the cooling rate is defined as crystallization rate parameter (CRP) and a higher slope indicates faster crystallization rate.[23,24] Figure 4 shows plots of $1/t_{1/2}$ as a function of cooling rate. The CRP values for neat PBT, PBT/FVAR1, PBT/FVAR3, and PBT/FVAR6 were respectively 0.071, 0.067, 0.058, and 0.50 K^{-1}.

Avrami model

Avrami equation[25–35] can be used to describe the primary stage of nonisothermal crystallization. The Avrami equation is expressed as:

$$X_t = 1 - \exp\left(-(K_a t)^{n_a}\right) \tag{3}$$

where X_t is the relative crystallinity, t is crystallization time, K_a is the Avrami crystallization rate constant and n_a is the Avrami exponent. X_t can be calculated as the ratio between the area of the exothermic

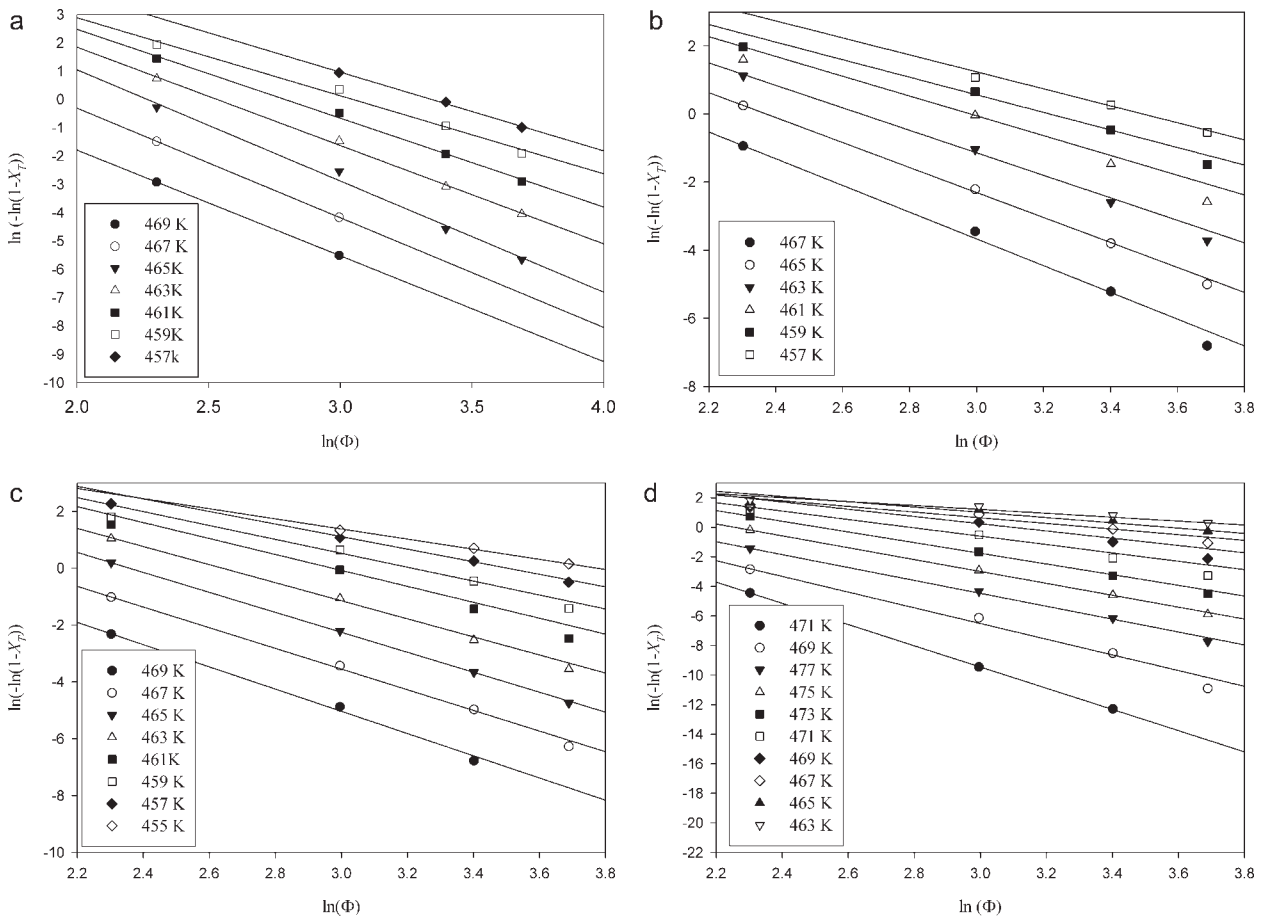

Figure 5 Ozawa analysis based on the nonisothermal crystallization of PBT and PBT/FVAR blends. (a) PBT, (b) PBT/FVAR1, (c) PBT/FVAR3, (d) PBT/FVAR6.

TABLE III
Ozawa Kinetic Parameters

Sample	Temperature (K)	n_o	K_o	R^2
PBT	457	2.79	28.9326	0.9926
	459	2.99	22.3331	0.9902
	461	3.04	16.8417	0.9925
	463	3.33	12.5103	0.9992
	465	3.61	9.2633	0.9975
	467	4.00	6.9500	0.9958
	469	5.37	5.8057	1.0000
PBT/FVAR1	457	2.49	33.0556	0.9799
	459	2.57	25.0071	0.9777
	461	2.91	19.7361	0.9572
	463	3.30	14.2301	0.9953
	465	3.66	10.7195	0.9992
	467	3.92	7.8932	0.9955
PBT/FVAR3	455	1.78	43.6017	0.9967
	457	2.21	33.2354	0.9786
	459	2.448	24.8898	0.9695
	461	2.80	19.5418	0.9623
	463	3.18	14.0255	0.9720
	465	3.51	10.5727	0.9998
	467	3.63	7.5720	0.9986
	469	3.91	5.5433	0.9972
PBT/FVAR6	453	1.32	50.2770	0.9539
	455	1.78	35.5072	0.9280
	457	1.912	28.203	0.9100
	459	2.45	22.1843	0.9230
	461	2.83	16.2552	0.9649
	463	3.61	12.3470	0.9982
	465	4.02	9.5486	0.9996
	467	4.36	7.2167	0.9984
	469	5.31	5.8966	0.9911
	471	7.21	1.1833	0.9999

peak at time t and the total measured area of crystallization. Values of K_a and n_a were found by fitting experimental data of X_t to eq. (3) and the results were shown in Table II.

In nonisothermal crystallization, because temperature changes constantly, K_a and n_a do not have the same physical significance as in the isothermal crystallization. This temperature changes affect the rate of both nuclei formation and spherulite growth. However, eq. (3) provided a good fit to experimental data based on regression coefficient (R^2).

Jeziorny[36] assumed constant or approximately constant cooling rate and proposed the final form of the parameter characterizing the kinetics of nonisothermal crystallization:

$$\ln K_J = \frac{\ln K_a}{\Phi} \tag{4}$$

The values of K_J were listed in Table II. K_J increased with increasing cooling rate for all samples.

Ozawa model

Considering the effect of cooling rate on the nonisothermal crystallization, Ozawa modified the Avrami model from isothermal crystallization to the nonisothermal crystallization by assuming that crystallization occurs at a constant cooling rate and the model as following[37]:

$$X_T = 1 - \exp\left[-\left(\frac{K_o}{\Phi}\right)^{n_o}\right] \tag{5a}$$

$$\ln\{-\ln[1 - X_T]\} = \ln K_o - n_o \ln \Phi \tag{5b}$$

where K_o and n_o are Ozawa crystallization rate constant and Ozawa exponent, respectively. Figure 5 illustrates the plots of ln [−ln (1 − X_T)] as a function of ln Φ for a fixed temperature. The K_o and n_o could be estimated from the y-intercept [(K_o =exp (y − intercept/n_o)] and slope. The Ozawa kinetic parameters as well as regression coefficient (R^2) were listed in Table III. Figure 5 and regression coefficient (R^2) listed in Table III showed that Ozawa model provided a satisfactory fit to the experimental data of both samples studied. Ozawa exponent n_o was found to range from 2.79 to 5.37 for neat PBT within 457–469 K, from 2.49 to 3.92 for PBT/FVAR1 within 457–467 K, from 1.78 to 3.91 for PBT/FVAR3 within 455–469 K, and from 1.32 to 7.21 for PBT/FVAR6 within 453–471 K. n_o increased with increasing crystallization temperature indicating the change of nucleation during the crystallization process.[38,39]

Liu model

Liu et al.[40] combined Avrami and Ozwa models to deal with the nonisothermal crystallization behavior and its form is given as follow:

$$\ln \Phi = \ln\left[\frac{K_o^{n_o}}{K_a^{n_a}}\right]^{1/n_0} - \frac{n_a}{n_o}\ln t \tag{6a}$$

$$F(T) = \left[\frac{K_o^{n_o}}{K_a^{n_a}}\right]^{1/n_o} \tag{6b}$$

$$a = \frac{n_a}{n_o} \tag{6c}$$

where the kinetic parameter, $F(T)$, refers to the value of the cooling rate chosen at the unit crystallization time when the measured system amounts to a certain degree of crystallinity; a is the ratio of Avrami exponent (n_a) to the Ozawa exponent (n_o). At a given degree of crystallinity, plotting ln Φ versus ln t (Fig. 6) yielded a linear relationship between ln Φ and ln t and the values of $F(T)$ and a (Table IV) could be obtained from the slopes and intercepts of these lines, respectively. The value of a varied from 1.53 to 1.71 for neat PBT, 1.45 to 1.55 for PBT/FVAR1, 1.48

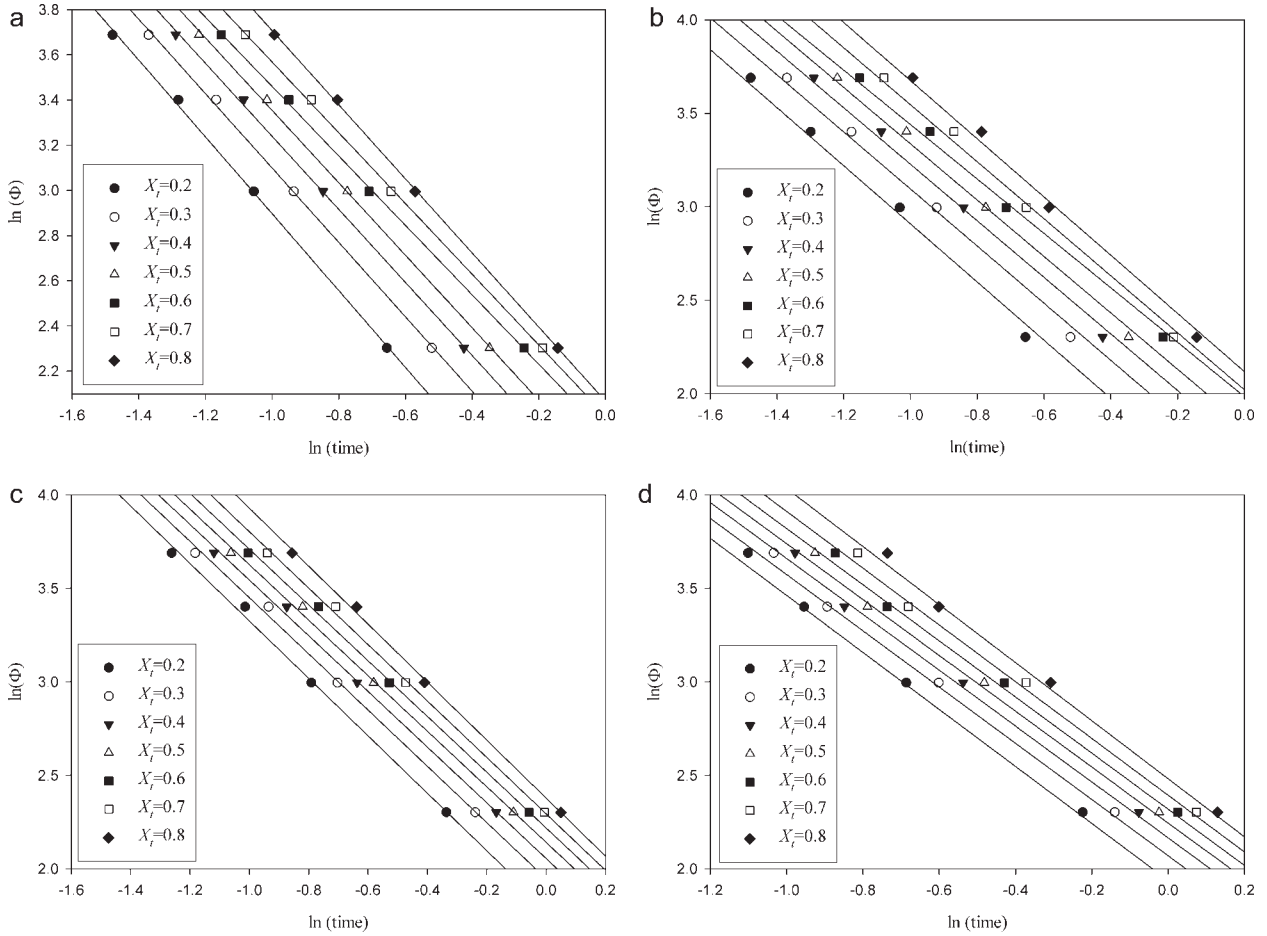

Figure 6 Plots of ln Φ versus ln t for different relative degree of crystallinity for PBT and PBT/FVAR blends. (a) PBT, (b) PBT/FVAR1, (c) PBT/FVAR3, (d) PBT/FVAR6.

to 1.55 for PBT/FVAR3 and 1.49 to 1.55 for PBT/FVAR6. The value of *F(T)* increased with increasing degree of crystallinity indicating that at unit crystallization time, a higher cooling rate was required to reach a higher degree of crystallinity. At the same relative degree of crystallinity, the value of *F(T)* for PBT was lower than those for PBT/FVAR blends; that is, to reach the same relative degree of crystallinity, PBT required lower cooling rate, which indicated that neat PBT crystallized faster than PBT/FVAR blends.

Comparison of kinetic models

These three models (Avrami, Ozawa, and Liu) provided simulated fit to experimental data. Avrami model has provided a simple method to ''describe'' a nonisothermal crystallization process although the physical meanings of its kinetic parameters (K_a and n_a) are not yet clear.[25–27] Figure 4 show the predicted curves based on the Avrami model (shown as solid lines), versus the experimental, it indicates that Avrami model provides good fitting below X_t = 0.8. It is difficult, however, for Ozawa and Liu models to reconstruct the nonisothermal crystallization process with those kinetic parameters (e.g. Fig. 3). To be able to simulate a nonisothermal process is of great interest because industrial operations involve mostly nonisothermal crystallization.

Ozawa has extended the Avrami theory to a nonisothermal case by assuming a constant cooling rate when the sample is cooled from the molten state. Similar to the Avrami exponent, the Ozawa exponent depends on the nucleation and growth mechanisms. Ozawa treatment is essentially quasi-isothermal in nature. The X_t chosen at a given temperature include the values on the earliest stage as well as the values from the end stage of crystallization due to variation in the cooling rates. When the cooling rates vary in a wide range, the selected X_t values may have included secondary crystallization. Furthermore, nonisothermal crystallization is a dynamic process in which the crystallization rate is no longer constant but a function of time and cooling rate. Also, nucleation may be more complicated than that of isothermal crystallization. These factors have

TABLE IV
Value of *F(T)* and *a* for PBT and PBT/FVAR Blends

Sample	X_t	$F(T)$	a	R^2
PBT	0.2	3.27	1.71	0.9939
	0.3	4.24	1.65	0.9993
	0.4	5.03	1.62	0.9994
	0.5	5.73	1.61	0.9994
	0.6	6.86	1.53	0.9995
	0.7	7.42	1.56	0.9996
	0.8	7.90	1.64	0.9997
PBT/FVAR1	0.2	3.85	1.55	0.9695
	0.3	4.75	1.52	0.9611
	0.4	5.55	1.51	0.9713
	0.5	6.22	1.50	0.9709
	0.6	7.27	1.45	0.9799
	0.7	7.45	1.52	0.9768
	0.8	8.31	1.55	0.9793
PBT/FVAR3	0.2	5.98	1.53	0.9980
	0.3	7.00	1.50	0.9977
	0.4	7.80	1.49	0.9981
	0.5	8.50	1.48	0.9983
	0.6	9.18	1.48	0.9985
	0.7	9.90	1.50	0.9987
	0.8	10.78	1.55	0.9988
PBT/FVAR6	0.2	6.93	1.52	0.9770
	0.3	7.92	1.50	0.9808
	0.4	8.71	1.49	0.9828
	0.5	9.44	1.49	0.9839
	0.6	10.15	1.50	0.9846
	0.7	10.94	1.51	0.9849
	0.8	11.95	1.55	0.9842

made the quasi-isothermal nature of Ozawa treatment somewhat questionable.

Liu model combines Avrami and Ozawa models, where the physical meaning of the rate parameter $F(T)$ refers to the necessary value of cooling rate to reach a defined degree of crystallinity at unit crystallization time. The good linearity of the plots (ln R against ln t) verifies the advantage of the combined approach applied.

All kinetic parameters from these models [K_J, K_o, and $F(T)$] predicted that the ''crystallization rate'' followed the order : PBT > PBT/FVAR1 > PBT/FVAR3 > PBT/FVAR6 at a given cooling rate during experimental crystallization. However, to compare the crystallization ability, undercooling should be taken into consideration when samples with different equilibrium temperatures (T_m^o), since the crystallization rate of a polymer depends mainly on its undercooling.[41] In previous study, the equilibrium temperatures of these four samples were estimated by nonlinear Hoffman–Weeks equation ($T_m^{o\mathrm{NLHW}}$) and listed in Table V. Figure 7 shows the undercooling needed to be imposed to reach 50% relative crystallization ($X_t = 0.5$), that is $T_m^{o\mathrm{NLHW}} - T_{1/2}$. The undercooling followed the order: PBT/FVAR1 > PBT/FVAR3 > PBT/FVAR6 > PBT, and it indicated that the crystallization ability followed the order: PBT > PBT/FVAR6 > PBT/FVAR3 > PBT/FVAR1. The results suggested that the addition of FVAR will hinder crystallization; however, more content of FVAR induces more heterogeneous nuclei and increased the crystallization ability. The results from nonisothermal crystallization were similar to those from isothermal crystallization in previous study.

Lauritzen–Hoffman equation

Lim[42] modified the Lauritzen–Hoffman equation to measure the spherulite growth rate as a function of temperature and cooling rate in nonisothermal crystallization as following equation:

$$\ln G + \frac{U^*}{R(T_o - \Phi t - T_\infty)} = \ln G_o - \frac{K_g}{(T_o - \Phi t)[T_m^o - (T_o - \Phi t)]f} \quad (7a)$$

$$f = \frac{2(T_o - \Phi t)}{T_m^o + (T_o - \Phi t)} \quad (7b)$$

G is the growth rate and is approximated as $1/t_{1/2}$ (i.e., $t = t_{1/2}$)[43]; G_o is the pre-exponential factor; $U^*$is the diffusional activation energy for the transport of crystallizable segments at the liquid–solid interface; R is the gas constant; $T_\infty = T_g - 30$ K is the hypothetical temperature below which viscous flow ceases and T_g is glass transition temperature of PBT and $T_g = 248$ K[44,45]; K_g is the nucleation parameter, which can be related to the product of lateral and folding surface free energy. Figure 8 shows the linear plot of eq. (7) for PBT, PBT/FVAR1, PBT/FVAR3, and PBT/FVAR6 by using $T_m^o = T_m^{o\mathrm{NLHW}}$. The K_g could be obtained from the slope of Figure 8 and the results are listed in Table V. The higher value of K_g in PBT/FVAR blends than neat PBT indicated the addition of FVAR reduces the mobility of polymer chains during crystallization although

TABLE V
Lauritzen–Hoffman Analyses for Nonisothermal Crystallization of PBT and PBT/FVAR Blends

	PBT	PBT/FVAR1	PBT/FVAR3	PBT/FVAR6
T_m^o (K)	$T_m^{o\mathrm{NLHW}}$ 32	$T_m^{o\mathrm{NLHW}}$ 77	$T_m^{o\mathrm{NLHW}}$ 558	$T_m^{o\mathrm{NLHW}}$534
K_g (10^{-5}, K^2)	2.8	10.4	6.8	3.1
R^2	0.9701	0.9999	0.9995	0.9647

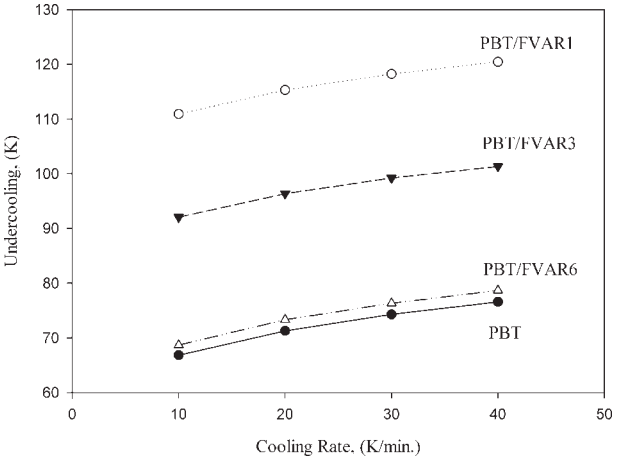

Figure 7 Undercooling to reach 50% relative crystallinity for PBT and PBT/FVAR blends at various cooling rate.

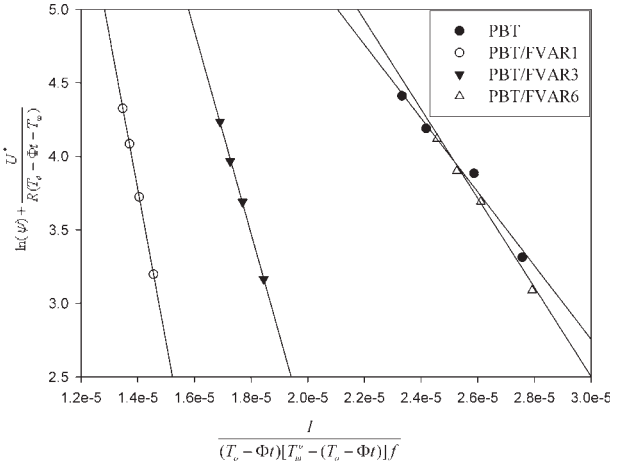

Figure 8 Modified Lauritzen–Hoffman type plots constructed from nonisothermal crystallization rate data.

FVAR increases the nucleation rate. The addition of more FVAR (PBT/FVAR3 and PBT/FVAR6) into the PBT matrix caused more heterogeneous nucleation and to obtain a lower K_g. The value of K_g in PBT/FVAR3 and PBT/FVAR6 was lower than that of PBT/FVAR1, which implies that the presence of more content of FVAR induces more heterogeneous nuclei and facilitate the crystallization*. Comparing the corresponding values for K_g from isothermal crystallization in previous study and nonisothermal crystallization, the values of K_g show similar trend: PBT/FVAR1 > PBT/FVAR3 > PBT/FVAR6 > PBT.

Effective energy barrier

Some methods have been suggested to estimate the effective energy barrier in nonisothermal crystallization.[46–48] However, to drop the negative sign in cooling process may result in errors.[49] The Friedman equation[50] is applied to nonisothermal crystallization for estimating the dependence of the effective activation energy on conversion and temperature. The Friedman equation can be expressed as follows:

$$\ln\left(\frac{dX_t}{dt}\right)_{X_t} = \text{constant} - \frac{\Delta E_{X_t}}{RT_{X_t}} \tag{8}$$

where dX_t/dt is the instantaneous crystallization rate as a function of time for a given value of the relative crystallinity (X_t), R is the universal gas constant, and ΔE_{X_t} is the effective energy barrier of the process for a given value of X_t. At various cooling rates, the values of dX_t/dt at a specific X_t are correlated to the corresponding crystallization temperature at this X_t, that is, T_{X_t}, a straight line can be obtained by plotting dX_t/dt versus $1/T_{X_t}$ and the slope is $-\Delta E_{X_t}/R$.

The dependence of the effective activation energy on conversion, which is based on Friedman equation, was shown in Figure 9. The activation energy increased with the increase in the relative crystallinity in all samples. At lower X_t, the PBT/FVAR blends showed lower activation energy than neat PBT; however, at higher X_t, PBT/FVAR blends showed higher activation energy. It may be ascribed to that FVAR particles acted as nucleating agents to facilitate the crystallization, however, hindered the crystallization at higher X_t.

CONCLUSIONS

DSC isothermal results reveal that introducing FVAR particles into the PBT causes a change of the crystal growth process. The nonisothermal crystallization behavior of neat PBT and PBT/FVAR blends was studied by DSC and by kinetic models. All kinetic parameters [K_J, K_o, and $F(T)$] showed that the ''crystallization rate'' followed the order: PBT > PBT/FVAR1 > PBT/FVAR3 > PBT/FVAR6 at a given cooling rate during experimental crystallization.

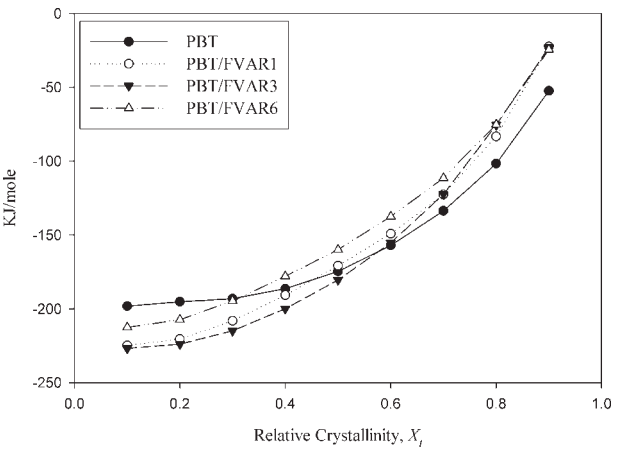

Figure 9 Dependence of the effective energy barrier on the extent of relative crystallinity.

However, when undercooling was taken into consideration, crystallization ability followed the order: PBT > PBT/FVAR6 > PBT/FVAR3 > PBT/FVAR1. The results suggest that the addition of FVAR will hinder crystallization; however, more content of FVAR induces more heterogeneous nuclei and increases the crystallization ability. Nucleation parameter (K_g) derived from a modified the Lauritzen–Hoffman equation also showed the same trend. Activation energy obtained from Friedman equation showed that the PBT/FVAR blends had lower activation energy than neat PBT at lower X_t because FVAR particles acted as nucleating agents to facilitate the crystallization; however, PBT/FVAR blends had higher activation energy at higher X_t because FVAR particles hindered the crystallization.

References

1. Sun, S. L.; Tan, Z. Y.; Zhang, M. Y.; Yang, M. D.; Zhang, H. X. Polym Int 2006, 55, 834.
2. Arostegui, A.; Gaztelumedi, M.; Nazabal, J. Polymer 2001, 42, 9565.
3. Hale, W.; Keskkula, H.; Paul, D. R. Polymer 1999, 40, 365.
4. Hale, W.; Keskkula, H.; Paul, D. R. Polymer 1999, 40, 3665.
5. Hale, W. R.; Pessan, L. A.; Keskkula, H.; Paul, D. R. Polymer 1999, 40, 4237.
6. Hale, W.; Lee, J. H.; Keskkula, H.; Paul, D. R. Polymer 1999, 40, 3621.
7. Wang, H. X.; Zhang, H. X.; Wang, Z. G.; Jiang, B. Z. Polymer 1997, 38, 1569.
8. Cecere, A.; Greco, R.; Ragosta, G.; Scarinzi, G.; Taglialatela, A. Polymer 1990, 31, 1239.
9. Zhang, H. X.; Hourston, D. J. J Appl Polym Sci 1999, 71, 2049.
10. Arostegui, A.; Nnazabal, J. J Polym Sci Part B: Polym Phys 2003, 41, 2236.
11. Liu, Y.; Zhang, X.; Wei, G.; Gao, J.; Huang, F.; Zhang, M.; Guo, M.; Qiao, J. Chin J Polym Sci 2002, 20, 93.
12. Qiao, J.; Zhang, X.; Liu, Y.; Wei, G.; Zhang, S. H.; Zhang, M.; Gao, J.; Huang, F. Symposium of Polymer Science of China 2001, G-243.
13. Wu, S. J Appl Polym Sci 1988, 35, 549.
14. Huang, J. W. Eur Polym, submitted.
15. DiLorenzo, M. L.; Silvestre, C. Prog Polym Sci 1999, 24, 917.
16. Hay, J. N.; Sabir, M. Polymer 1969, 10, 203.
17. Hay, J. N.; Fitzgerald, P. A.; Wiles, M. Polymer 1976, 17, 1015.
18. Fatou, J. G. Makromol Chem 1984, 7, 131.
19. Zhang, G.; Yan, D. J Appl Polym Sci 2003, 88, 2181.
20. Ma, C. C.; Kuo, C. T.; Kuan, H. C.; Chiang, C. L. J Appl Polym Sci 2003, 88, 1686.
21. Jimenez, C. G.; Ogata, N.; Kawai, H.; Ogihara, T. J Appl Polym Sci 1997, 64, 2211.
22. Weng, W.; Chen, G.; Wu, D. Polymer 2003, 44, 8119.
23. Zhang, U.; Zheng, H.; Lou, X.; Ma, D. J Appl Polym Sci 1994, 51, 51.
24. Supaphol, P.; Dangseeyun, N.; Srimoaon, P. Polym Test 2004, 23, 175.
25. Supaphol, P.; Lin, J. S. Polymer 2001, 42, 9617.
26. Supaphol, P. J Appl Polym Sci 2000, 78, 338.
27. Supaphol, P.; Dangseeyun, N.; Srimoaon, P.; Nithitanakul, M. Thermochim Acta 2003, 406, 207.
28. Vyazovkin, S.; Sbirrazzuoli, N. J Phys Chem B 2003, 107, 882.
29. Kolmogorov, A. N. Izv Akad Nauk USSR Ser Math 1937, 1, 355.
30. Johnson, W. A.; Mehl, K. F. Trans Am Inst Mining Metall Eng 1939, 135, 416.
31. Avrami, M. J. Chem Phys 1939, 7, 1103.
32. Avrami, M. J. Chem Phys 1939, 8, 212.
33. Avrami, M. J. Chem Phys 1939, 9, 177.
34. Evans, U. R. Trans Faraday Soc 1945, 41, 365.
35. Ding, Z; Spruiell, J. E. J Polym Sci Part B: Polym Phys 1997, 35, 1077.
36. Jeziorny, A. Polymer 1978, 19, 1142.
37. Ozawa, T. Polymer 1971, 12, 150.
38. Qui, Z.; Fujinami, S.; Komura, M.; Nakajima, K.; Ikehara, T.; Nishi, T. Polym J 2004, 36, 642.
39. Somrang, N.; Nithitanakul, N.; Grady, B. P.; Supaphol, P. Euro Polym J 2004, 40, 829.
40. Liu, T. X.; Mo, Z. S.; Wang, S. E.; Zhang, H. F. Polym Eng Sci 1997, 37, 568.
41. DiLorenzo, M. L.; Silvestre, C. Prog Polym Sci 1999, 24, 917.
42. Lim, B. A.; McGuire, K. S.; Lloyd, D. R. Polym Eng Sci 1993, 33, 537.
43. Achilias, D. S.; Papageorgiou, G. Z.; Karayannidis, G. P. J Polym Sci Part B: Polym Phys 2004, 42, 3775.
44. Cheng, S. Z. D.; Pan, R.; Wunderlich, B. Makromol Chem 1988, 18, 2443.
45. Dilorenzo, M. L.; Righetti, M. C. Polym Eng Sci 2003, 43, 1889.
46. Augis, J. A.; Bennett, J. E. Therm Anal 1978, 13, 283.
47. Kissinger, H. E. J Res Natl Bur Stand 1956, 57, 217.
48. Takhor, R. L. Advances in Nucleation and Crystallization of Glasses; American Chemical Society: Columbus, 1971.
49. Vyazovkin, S.; Sbirrazzuoli, N. J Phys Chem B 2003, 107, 882.
50. Friedman, H. J Polym Sci Part C: Polym Symp 1964, 6, 183.